

## TAMARIND SEEDS CARBON: PREPARATION AND METHANE UPTAKE

K. Munusamy, Rajesh S. Somani, and Hari C. Bajaj \*

Tamarind seeds carbon (TSC) from tamarind (*Tamarindus indica*) seeds, an agro-byproduct and waste that is available abundantly in the southern states of India, was prepared by chemical activation with KOH. The influence of tamarind seeds char to KOH weight ratio (1:1 to 1:4) and activation temperature (400 to 800 °C) were investigated. TSC having micro-pore volume as high as 1.0 cm<sup>3</sup>/g with surface area 2673 m<sup>2</sup>/g was obtained. TSC was characterized by scanning electron microscopy, powder X-ray diffraction analysis, thermogravimetric analysis, and FT-IR spectroscopy. The potential of TSC to be used as a methane storage material was tested and compared with a commercial activated carbon. The highest methane adsorption capacity obtained for TSC was ca. 32.5 cm<sup>3</sup>/g at 30 °C and 1 bar. The maximum methane storage capacity achieved was 180 cm<sup>3</sup>/g at 30 °C and 35 bars.

*Keywords:* Tamarind seeds; Activated carbon; Chemical activation; Methane storage; Adsorption

*Contact information:* Discipline of Inorganic Materials and Catalysis, Central Salt and Marine Chemicals Research Institute, Council of Scientific & Industrial Research (CSIR), G. B. Marg, Bhavnagar - 364 021, Gujarat, India; \* Corresponding author: hcbajaj@cscri.org

### INTRODUCTION

India is the major producer of tamarind (Botanical name: *Tamarindus indica* L.) on a commercial scale. Thailand has the largest plantations of the ASEAN nations, followed by Indonesia, Myanmar, and the Philippines. Tamarind, the fruit of a tropical tree, also known as “date of India” is actually the fruit pod produced by a tall, semi-evergreen tree grown primarily in India. Tamarind is an important adjunct/condiment used as a sour ingredient in Indian cookery. India produces about 0.25 million tonnes of tamarind pulp per annum (NRDC Technology offer- Website: [www.nrdcindia.com](http://www.nrdcindia.com), TAMARIND POWDER.htm). The tree produces brown pod-like fruits, which contain pulp and hard-coated seeds. The fully formed seeds are hard, glossy-brown, and square shaped with rounded corners and edges; each is enclosed in a parchment. A mature tree may annually produce 150 to 225 kgs of fruits, of which the pulp may constitute 30 to 55%, the shells and fiber, 11 to 30%, and the seeds, 33 to 40%. Thus, a large quantity of tamarind seeds is available as agro-byproduct or waste.

There are several reports on the preparation of Activated Carbon (AC) from agro-byproducts or wastes, which include a number of nutshells such as oil palm shell (Arami-Niya et al. 2010; Daud and Ali 2004), almond shell (Rodriguez-Reinoso and Molina-Sabio 1992; Gergova et al. 1994; Balsi et al. 1994), coconut shell (Gratuito et al. 2008; Laine and Calafat 1991; Pandolfo et al. 1994), pistachio shells (Yang and Lua 2006), hazelnut shell (Balsi et al. 1994), and other by-products such as olive stones (Nakagawa

et al. 2007), date stones (Bouchelta et al. 2008), rice bran (Suzuki et al. 2007), coffee residue (Boonamnuayv et al. 2005), apricot stones (Sentorun-Shalaby et al. 2006), peach and cherry stones (Rodriguez-Reinoso and Molina-Sabio 1992; Gergova et al. 1994; Caturla et al. 1991), grape seeds (Gergova et al. 1994), and rubberwood saw dust (Srinivasa Kannan and Abu Bakar 2004). Activated carbon prepared from agricultural wastes was used to study the adsorption kinetics of Cr(VI) from aqueous solution (Kobya et al. 2004). Rice bran carbon was also used for the removal of hexavalent chromium (Ranjan et al. 2010). The use of such starting materials contributes significantly to reduce solid waste and the production cost of AC. AC with high surface area and porosity are widely used for the gas separation and purification as well as removal of organic and inorganic contaminants from polluted water streams.

The chemical activation method is widely used for the preparation of AC. In this method, raw material impregnated with an activating agent is calcined in an inert atmosphere. The carbonization and activation steps progress simultaneously in this method. The chemicals used as an activating agent are KOH, NaOH, Na<sub>2</sub>CO<sub>3</sub>, K<sub>2</sub>CO<sub>3</sub>, H<sub>3</sub>PO<sub>4</sub>, and ZnCl<sub>2</sub>. They are dehydrating agents that influence pyrolysis decomposition and inhibit the formation of tar, enhancing the yield of AC (Bansal et al. 1988; Byrne and Marsh 1995; Moreno-Castilla et al. 2001). It has been reported that the resulting AC has the most favorable Natural Gas (NG) storage capacities (Golovoy 1983; Quinn 1994). Methane is the major component of NG.

The U. S. Department of Energy (DOE) has pursued a research programme on NG storage on porous materials. As evidenced by the published literature, much work has been done and is being carried out mainly on two classes of microporous materials: zeolites and activated carbons (Otto 1981; Matranga et al. 1992; Aukett et al. 1992; Parkyns et al. 1995; Quinn, 1992; Alcaniz-Monge et al. 1997; Chen et al. 1997; Menon et al. 1998; Vasil'ev et al. 1999; Rubel 2000). It has been shown that ACs are very good adsorbents, presenting the highest adsorbed natural gas (ANG) energy densities and thus the highest storage capacities (Cracknell 1993).

To the best of our knowledge, preparation of TSC and its potentiality as a methane storage material has not been reported earlier. Therefore, the present work aims to prepare TSC from tamarind seeds and to study the influence of tamarind seeds char to KOH weight ratio and activation temperature on its textural properties. The methane uptake of TSC was measured both at 1 and 35 bars and compared with a commercial activated carbon (WS-480, Calgon). TSC samples were further characterized by scanning electron microscopy (SEM), powder X-ray diffraction analysis (PXRD), thermogravimetric analysis (TGA), and FT-IR spectroscopy (FTIR).

## **EXPERIMENTAL**

### **Preparation of Carbon from Tamarind seeds**

Tamarind seeds are byproduct of tamarind pulp making plants and household use in Indian cookery. It was collected from the local market in Bhavnagar, Gujarat state, India. The outer layer of the seeds was removed, and the decoated seeds (T-pre) were charred at 300 °C for one hour under continuous flow of nitrogen (100 mL/min.). After

cooling the charred material (T-char) to ambient temperature, it was ground and passed through a 30 mesh screen and used as carbon source throughout the study. The sample of commercial activated carbon (WS-480, Calgon) was procured from Chemviron Carbon, Feluy, Belgium. Analytical reagent grade potassium hydroxide (KOH) was purchased from S.D. Fine Chemicals, Mumbai, India and used as a chemical activating agent.

For preparing activated carbon, the pre-dried T-char (5 grams) was mixed with KOH in the desired impregnation ratio (1:1 to 1:4) and 15 mL of distilled water in a plastic container. The mass was stirred at ambient temperature for 16 hr then transferred to a stainless steel vessel and heated to the desired activation temperature ( $T_{act} = 400$  to  $800$  °C) for 1 hr under the nitrogen flow (200 mL/min.). After completion of activation, the vessel was cooled to ambient temperature. The product was collected by washing the mass with distilled water until the filtrate was free from alkali.

### Characterization of Tamarind Seeds Carbon (TSC)

The textural properties of T-char and TSC were determined by  $N_2$  gas adsorption-desorption at  $-196$ °C method, using a surface area and pore size analyzer (Model ASAP-2020, Micromeritics Inc., U.S.A.). Total pore volume was determined by single-point adsorption at a partial pressure of 0.99, and the micropore volume was calculated by t-plot.

The pore size distributions were obtained by the MP method. Prior to the measurements, the TSC samples were degassed at  $300$  °C under high vacuum for 5 hr. The PXRD patterns of the TSC were obtained using a PHILIPS X'pert MPD system in the  $2\theta$  range of  $2$ -  $80$ ° using  $CuK\alpha_1$  ( $\lambda = 1.54056$  Å) radiation. The weight loss behaviors of the *Tamarindus indica* seeds and TSC were measured with a thermogravimetric analyzer (Mettler Toledo). The samples were heated up to  $800$  °C at a heating rate of  $10$  °C/min under nitrogen flow.

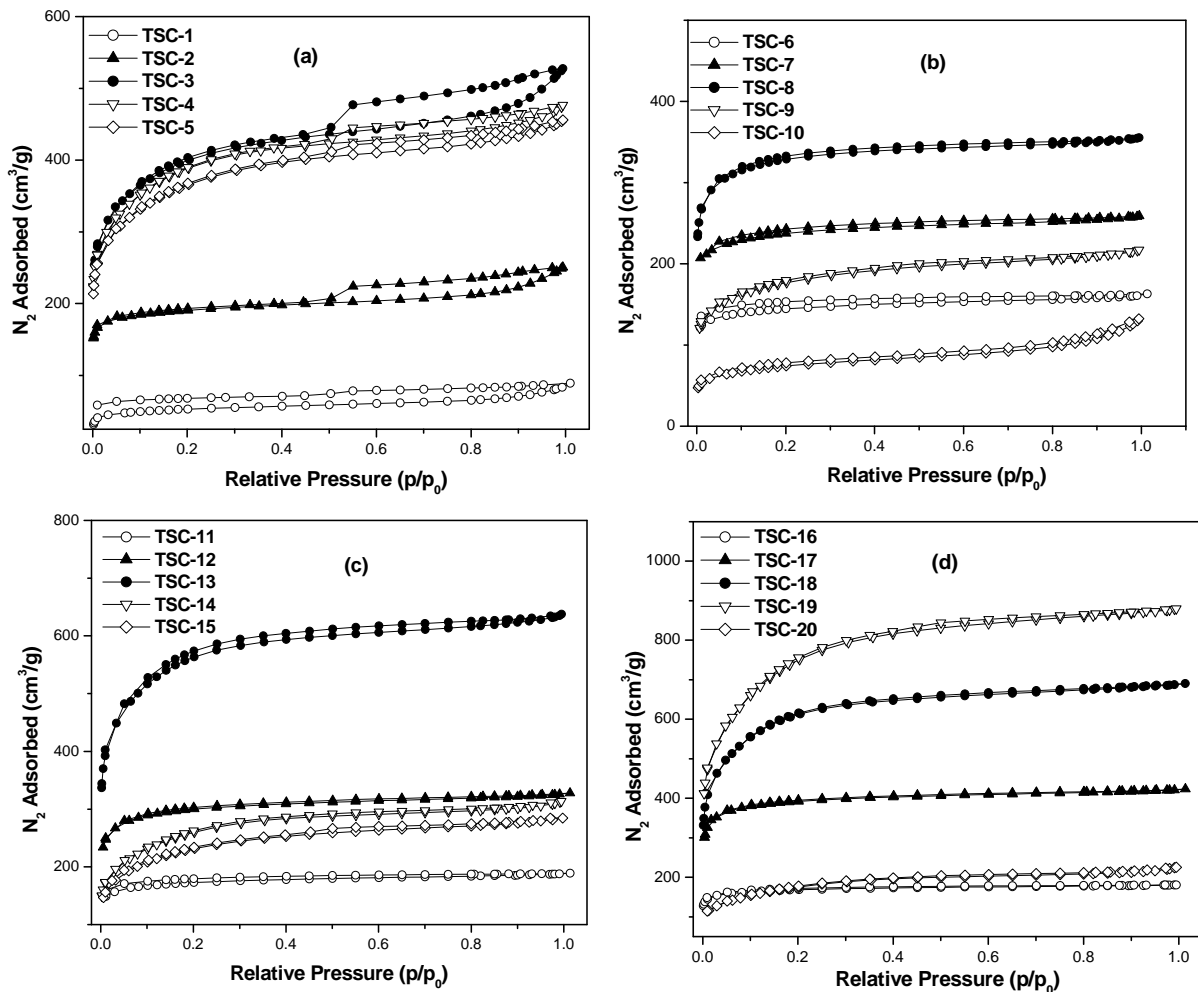
The morphology of tamarindus indica seeds and TSC were analyzed using a scanning electron microscope (SEM) LEO 1430. For elemental composition EDX analysis was performed using SEM. The surface functional groups were studied by Fourier transform infrared spectroscopy (Perkin Elmer, GX-FTIR). The spectra were recorded in the range  $4000$ - $400$   $cm^{-1}$ . High pressure methane adsorption data were collected using a BELSORP-HP system (BEL Inc., Japan).

## RESULTS AND DISCUSSION

The elemental composition of the decoated tamarind seeds (T-pre), T-char, and TSC sample obtained under optimized conditions (TSC-19) are given in Table 1. Table 1 shows that during the charring process, nitrogen containing components of decoated tamarind seeds (T-pre) are removed. TSC-19 contained 99.5% C, indicating that a high purity activated carbon can be produced from tamarind seeds.

**Table 1.** Elemental Composition of Decoated and Charred Tamarind seeds with Activated Carbon Derived from Tamarind Seeds

Sample name	By EDX			
	%C	%N	%O	%K
Decoated tamarind seeds (T-pre)	51.7	35.5	12.4	0.4
Charred tamarind seeds (T-char)	71.7	0.0	27.8	0.0
Tamarind seeds carbon (TSC-19)	99.5	0.3	0.0	0.2

**Fig. 1.** N<sub>2</sub> adsorption-desorption isotherms of tamarind seed carbons at T-char to KOH ratio (a) 1:1, (b) 1:2, (c) 1:3, and (d) 1:4

Figures 1(a-d) shows the nitrogen adsorption isotherms of TSC samples prepared at different T-char to KOH ratio and activation temperatures. All TSC samples showed an almost flat plateau at higher relative pressures and showed Type I isotherms. This

indicates the presence of microporous materials with a narrow pore size distribution. However, in the case of TSC-1 to TSC-5 hysteresis was observed in the higher relative pressures, indicating the presence of mesopores. The hysteresis was not observed for any other TSC samples. This indicated that at lower (1:1) T-char to KOH ratio formation of mesopores is favored. It was also observed that the mesoporosity increased with increase in activation temperature in the range 400 to 600°C. The shapes of isotherms indicate that the adsorption capacity for nitrogen increased with increasing activation temperature in the range 400 to 600°C and then it started decreasing at  $\geq 700$  °C. Moreover, the slope of plateau and the variation in the adsorption capacity were the major differences with other TSC samples, though its isotherms were of Type I. This indicates that the development of micro porosity was favored at lower ( $<700$ °C) activation temperatures for T-char to KOH ratio  $\geq 1:2$ . At higher ( $>700$  °C) activation temperatures due to high energy input in the form of heat some of the micropores might have been destroyed by collapse of pore walls creating larger micro pores raising the nitrogen adsorption and thereby increasing the surface area. The isotherms of TSC-7 and TSC-8 had different tendency at low relative pressure and parallel at relative pressure above  $p/p_0 = 0.3$ . This indicates that the differences were in the size of micropores. The isotherms of TSC-9 and TSC-10 showed similar tendency up to  $p/p_0 = 0.8$ . However, the nitrogen adsorption increased for TSC-10 at higher relative pressures indicating formation of mesopores.

The effect of activation temperature at different T-char to KOH weight ratio on surface area, total pore, and micropore volume of TSC samples is listed in Table 2 along with the methane uptake values at 30°C and 1 atm. The surface area values of TSC samples, prepared at 600°C activation temperature at different T-char to KOH ratio, were comparable with that of commercial sample WS-480. On the other hand, TSC-19 exhibited the highest surface area and micropore volume compared to all other TSC samples at activation temperature 700°C and T-char to KOH ratio 1:4. In general, as the activation temperature increased from 400 to 600°C the micropore volume also increased, reaching maximum value at 600°C. It can also be observed that all products except TSC-1, TSC-2, TSC-3, and TSC-10, showed low ( $<30\%$  of total pore volume) mesopores volume. Moreover, the total pore volume of TSC-3, TSC-4, TSC-5, TSC-13, TSC-18, and TSC-19 were higher compared with 0.68 cm<sup>3</sup>/g for commercial sample WS-480. In particular, TSC-19 and TSC-18 exhibited total pore volume as high as 1.36 and 1.06 cm<sup>3</sup>/g, respectively. Increase in both surface area and total pore volume from TSC-1 to TSC-3, TSC-6 to TSC-8, TSC-11 to TSC-13, and TSC-16 to TSC-19 is worth noticing. Though the microporosity of TSC-18 was on the higher side ( $V_{\text{micro}}/V_{\text{total}} = 83\%$ ), the surface area was lower (2147 m<sup>2</sup>/g). In contrast, TSC-19 had lower micro porosity (77%) with a higher surface area (2673 m<sup>2</sup>/g). The highest microporosity (89%) was observed for TSC-8, TSC-16, and TSC-17. The corresponding CH<sub>4</sub> uptake was 32.8, 17.2, and 31.5 cm<sup>3</sup>/g. On the other hand, the CH<sub>4</sub> uptake was highest (32.8 cm<sup>3</sup>/g) for TSC-8 and was very close (32.6 cm<sup>3</sup>/g) for TSC-19 and slightly lower (32.4 cm<sup>3</sup>/g) for TSC-18. The corresponding microporosity was 89%, 77%, and 83%. This indicated that a combination of textural properties govern the CH<sub>4</sub> uptake capacity of TSC samples. For obtaining CH<sub>4</sub> uptake at least 32 cm<sup>3</sup>/g, a combination of total pore volume (0.55 cm<sup>3</sup>/g) with micro porosity 89% and BET surface area ca. 1116 m<sup>2</sup>/g is required (e.g. TSC-8). The same CH<sub>4</sub> uptake capacity for TSC-18 can be achieved by a combination of total pore volume

(1.06 cm<sup>3</sup>/g) with micro porosity 83% and BET surface area ca. 2147 m<sup>2</sup>/g. As observed in case of TSC-19, a combination of total pore volume (1.36 cm<sup>3</sup>/g) with micro porosity 77% and BET surface area ca. 2673 m<sup>2</sup>/g resulted in > 32 cm<sup>3</sup>/g CH<sub>4</sub> uptake. To the best of our knowledge, the present work has produced activated carbons from tamarind seeds (TSC) with better micro porosity (as high as 89%), BET surface area (as high as 2673 m<sup>2</sup>/g), and total pore volume (as high as 1.36 cm<sup>3</sup>/g) compared to previously published biomass raw material based ACs.

Figures 2 (i-iv) show the pore size distribution of TSCs obtained at different T-char to KOH ratio and activation temperatures by MP method. It is apparent from Fig. 2 that the activation temperature and T-char to KOH ratio had significant effect on pore formation of the TSCs. All of the pore size distribution curves of TSCs had their maximum at the pore radius around 0.3 nm, except for the TSC-16 to TSC-19, which had a maximum at the pore radius 0.25 nm, signifying the presence of micropores.

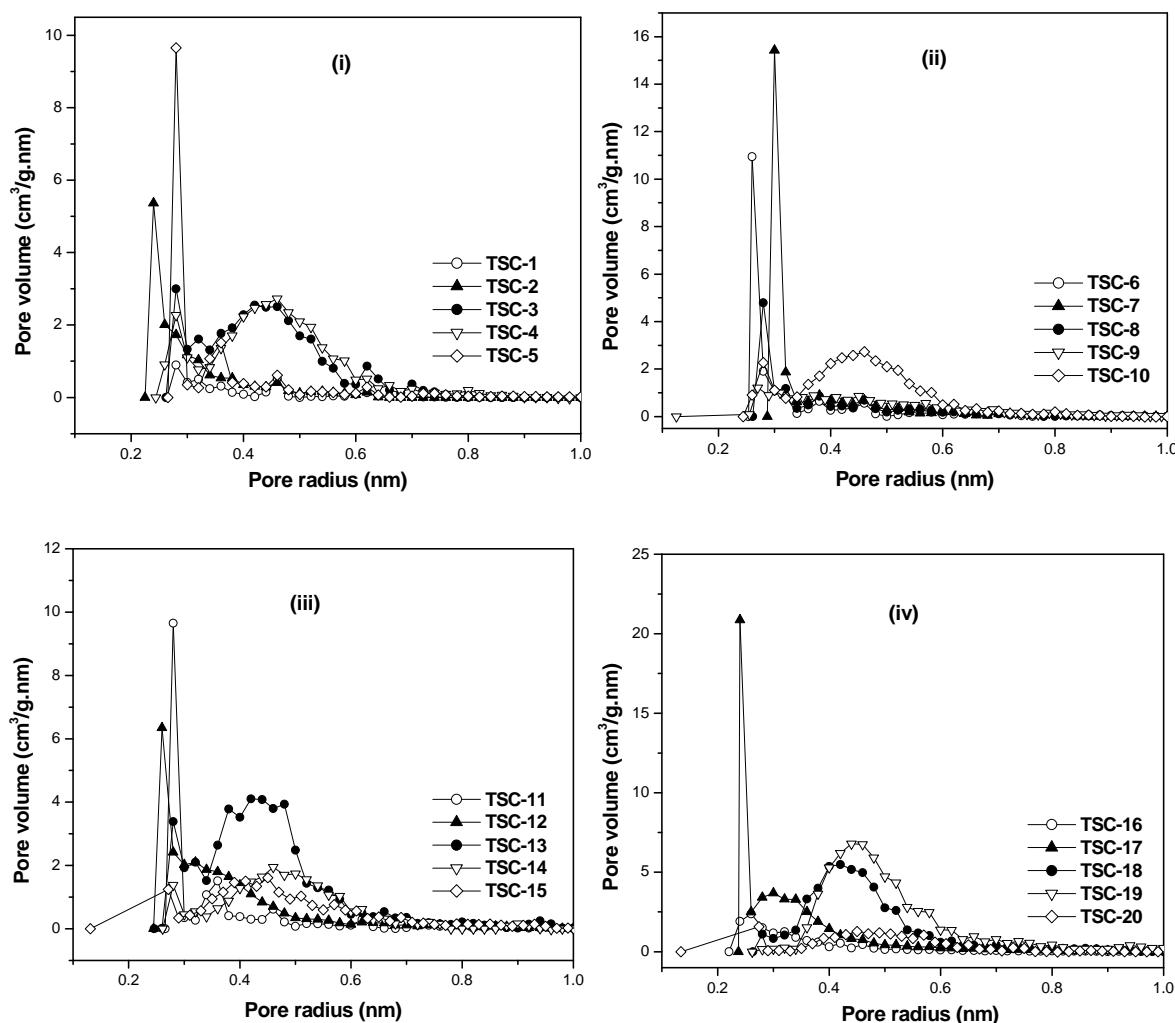


**Fig. 2.** Pore size distribution (MP method) of Tamarind seeds carbon prepared at different activation temperature and at T-char to KOH ratio (i) 1:1, (ii) 1:2, (iii) 1:3 and (iv) 1:4

TSC-3, TSC-4, TSC-10, TSC-13, TSC-14, TSC-15, TSC-18, and TSC-19 showed bimodal pore size distribution, as evidenced by the presence of a broad peak with maximum at the pore radius around 0.45 nm. This clearly indicated that when activation temperature increased at a particular T-char to KOH ratio the pores developed into a wider size distribution and the curves moved to a higher micropore size. The highest point of adsorption was in the pores with radius between 0.25 to 0.50 nm. This demonstrated that although the formation of micropores increased up to the activation temperature 600°C, widening of these micropores to a larger size occurred continuously in all the samples.

**Table 2.** Effect of Treatment on Textural Properties of Tamarind Seeds Carbon

Sample	Activation temperature (°C)	T-Char to KOH weight ratio	BET Surface area (m <sup>2</sup> /g)	Total pore volume (cm <sup>3</sup> /g)	Micro Pore volume (cm <sup>3</sup> /g)	CH <sub>4</sub> uptake (cm <sup>3</sup> /g) at 30°C, 1 bar
T-char	300	-	12	0.01	0.00	06.5
TSC-1	400	1:1	182	0.12	0.07	13.1
TSC-2	500	1:1	643	0.38	0.27	23.9
TSC-3	600	1:1	1391	0.79	0.55	24.0
TSC-4	700	1:1	1363	0.72	0.55	23.6
TSC-5	800	1:1	1277	0.69	0.50	22.4
TSC-6	400	1:2	488	0.25	0.21	22.1
TSC-7	500	1:2	800	0.40	0.35	28.8
TSC-8	600	1:2	1116	0.55	0.49	32.8
TSC-9	700	1:2	613	0.33	0.24	12.8
TSC-10	800	1:2	258	0.19	0.09	10.3
TSC-11	400	1:3	582	0.29	0.25	21.8
TSC-12	500	1:3	1016	0.50	0.44	25.9
TSC-13	600	1:3	1962	0.98	0.82	30.7
TSC-14	700	1:3	918	0.48	0.37	14.4
TSC-15	800	1:3	815	0.44	0.31	10.9
TSC-16	400	1:4	568	0.28	0.25	17.2
TSC-17	500	1:4	1325	0.65	0.58	31.5
TSC-18	600	1:4	2147	1.06	0.88	32.4
TSC-19	700	1:4	2673	1.36	1.05	32.6
TSC-20	800	1:4	625	0.34	0.24	11.4

The XRD patterns (Fig. 3) of tamarind seeds powder showed a sharp peak at  $2\theta = 20^\circ$  and a broad peak at  $42^\circ$ . The XRD patterns of the T-char and TSC-19 showed two broad peaks at around  $2\theta = 24^\circ$  and  $42^\circ$ . These peaks correspond to 100 and 002 planes usually observed for carbons. The broadness of the peaks indicated that these carbons were highly amorphous.

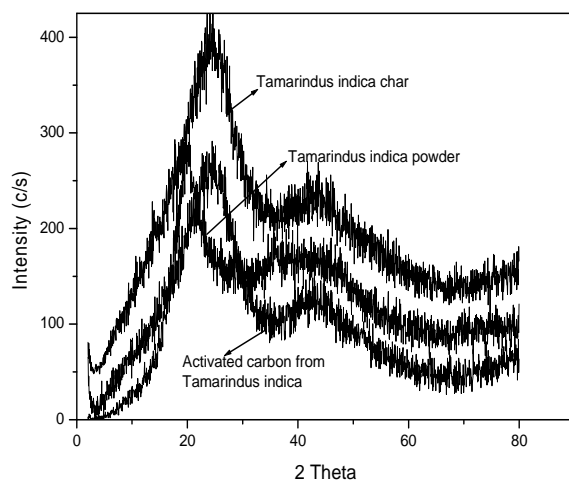


**Fig. 3.** PXRD patterns of a) tamarind seeds powder, b) tamarind seeds char, and c) activated carbon derived from tamarind seeds (TSC-19).

The major weight loss for tamarind seeds was observed between 220 and 350 °C during TGA analysis (Fig. 4), which may be due to the decomposition of polymeric network of cellulose and lignin, loss of water, carbon dioxide, and a wide range of organic molecules.

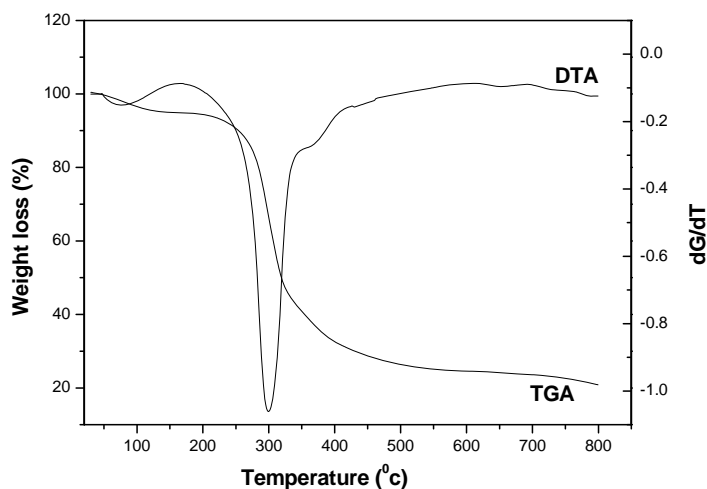


**Fig. 4.** Thermogravimetric (TGA) and differential thermal analysis (DTA) of tamarind seeds.

The SEM images (Fig. 5) showed that the decoated tamarind seeds were non-porous, whereas the T-char and TSC were porous. This can be attributed to the chemical activation using KOH, which plays the main role to develop and the formation of pores by the decomposition of water and other organic compounds.

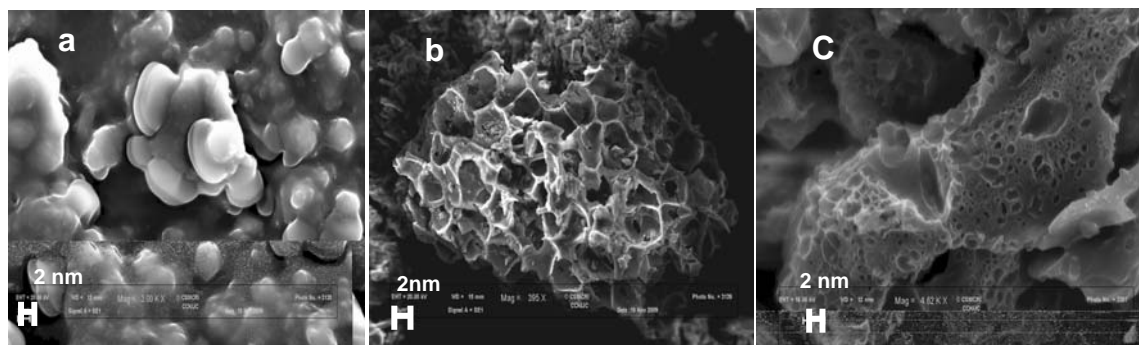


**Fig. 5.** SEM images of a) decoated tamarind seeds, b) tamarind seed char and c) activated carbon derived from tamarind seeds

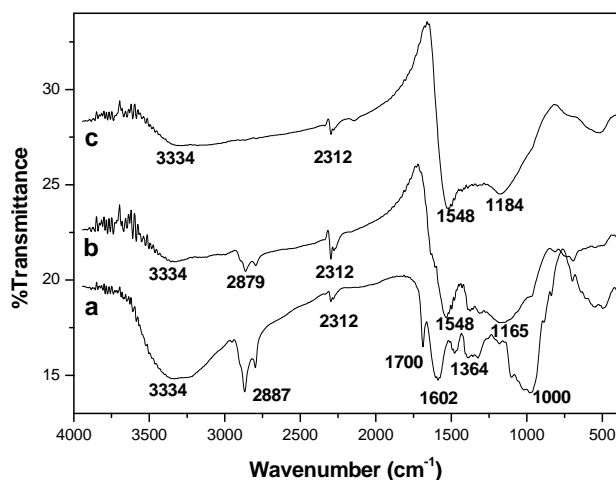


**Fig. 6.** FTIR spectra of a) decoated tamarind seeds (T-pre), b) tamarind seeds char (T-char), and c) activated carbon derived from tamarind seeds (TSC-19)

The IR spectra (Fig. 6c) of TSC-19 did not show the presence of any functional groups except a small peak at  $2312\text{ cm}^{-1}$  which is due to the atmospheric  $\text{CO}_2$ , and peaks observed at  $1548$  and  $1184\text{ cm}^{-1}$  are due to  $\text{C}=\text{C}$  and  $\text{C}-\text{C}$  stretching vibrations. Around  $3334\text{ cm}^{-1}$  a broad peak due to stretching vibrations of water/surface hydroxyl (OH) groups present in the T-pre (a), T-char (b), and TSC-19 (c) was observed. During the activation of char in the presence of KOH the formation and breakage of several bonds took place, which led to liberation and elimination of many organic compounds. This behavior is consistent with the disappearance of a band at  $1700\text{ cm}^{-1}$  in T-char and TSC-19, which is attributed to  $\text{C}=\text{O}$  present in the decoated tamarind seeds. A pair of bands in the range of  $2800$  to  $2900\text{ cm}^{-1}$  attributed to  $\text{C}-\text{C}$  is present in T-pre and T-char but disappeared in TSC-19. Peaks in the range  $800$  to  $1300\text{ cm}^{-1}$  are due to the presence of  $\text{C}-\text{O}$  stretching vibrations.

The methane adsorption isotherms of TSC samples (Fig. 7 a-d) and commercial sample WS-480 (Fig. 7e) were measured at  $30^\circ\text{C}$ . It was observed that all the isotherms were almost linear up to the relative pressure  $P/P_0 = 0.99$ . The highest methane adsorption

capacity obtained at T-char to KOH weight ratio 1:1, 1:2, and 1:3 was 24, 32.8, and 30.7  $\text{cm}^3/\text{g}$  respectively, prepared at activation temperature  $600^\circ\text{C}$ . On the other hand, the methane adsorption capacity was 31.5, 32.4, and  $32.6 \text{ cm}^3/\text{g}$  for TSC-17, TSC-18, and TSC-19 prepared using T-char to KOH weight ratio 1:4 at activation temperature 500, 600, and  $700^\circ\text{C}$ , respectively.

The methane adsorption isotherms up to 35 bars were measured at  $30^\circ\text{C}$  for selected TSC samples and are shown in Fig. 8. The methane adsorption capacities at 35 bars and  $30^\circ\text{C}$  of the TSC-3, TSC-8, TSC-13, TSC-18, TSC-19, and WS-480 were 99, 107, 116, 165, 180, and  $121 \text{ cm}^3/\text{g}$ , respectively. The bulk density of TSC-19 was determined to be  $0.3 \text{ g/cc}$ ; accordingly, the methane adsorption capacity is  $54 \text{ cc/cc}$ , which is much less than the DOE target of  $180 \text{ cc/cc}$ . Efforts are needed for the preparation of monoliths / shaped body using TSC and appropriate binders for improving the bulk density and also to achieve the methane sorption capacity. The  $\text{CH}_4$ -adsorption data up to 1 atm. and at  $30^\circ\text{C}$  were fitted into Langmuir equation, and it was found that it fitted very well as the values of the linear regression ( $R^2$ ) were between 0.97 and 0.99. The methane adsorptions on activated carbons derived from different sources are compiled in Table 3.

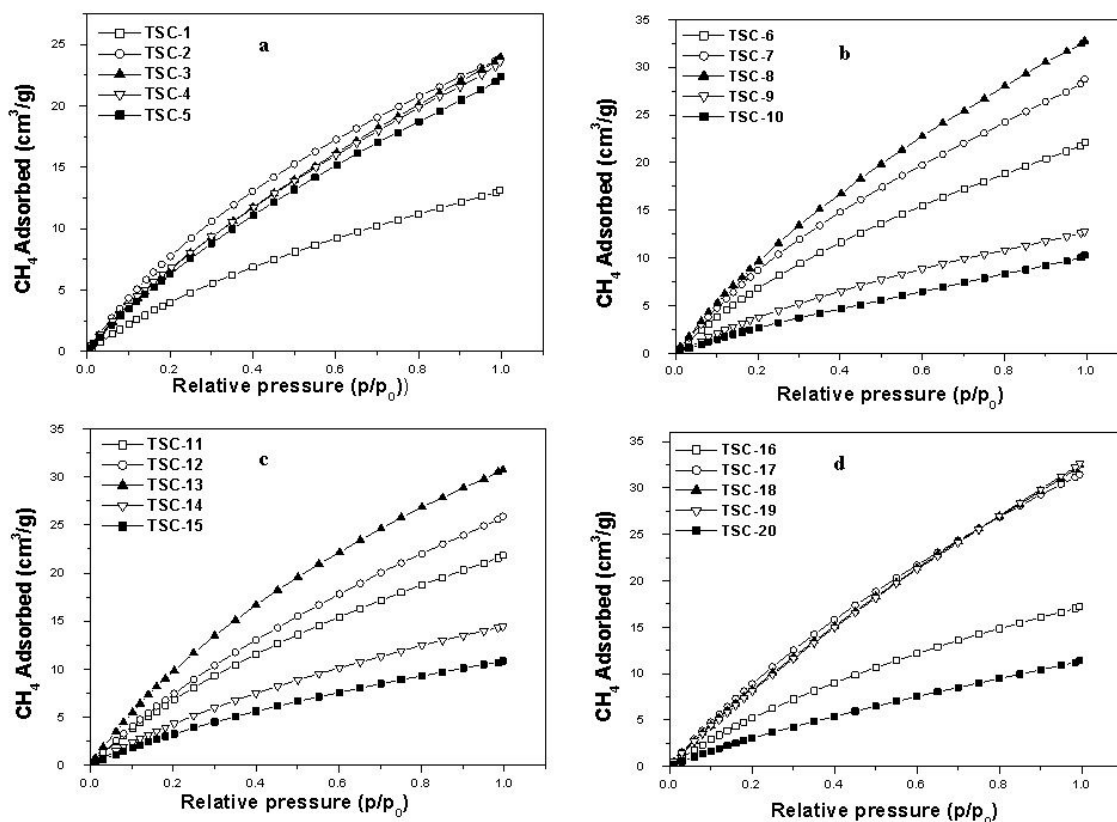


**Fig. 7 (a-d).** Methane adsorption isotherms at  $30^\circ\text{C}$  on activated carbon derived from tamarind seeds using different T-char to KOH weight ratio. a) 1:1, b) 1:2, c) 1:3, d) 1:4

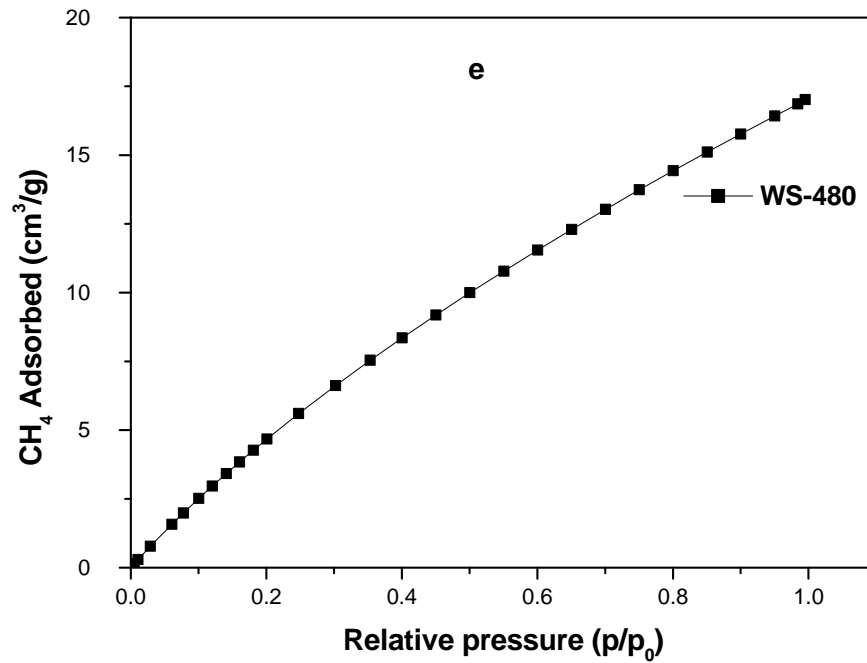


**Fig. 7e.** Methane adsorption isotherms at 30 °C on activated carbon derived from tamarind seeds using different T-char to KOH weight ratio. a) 1:1, b) 1:2, c) 1:3, d) 1:4 and e) commercial activated carbon WS-480

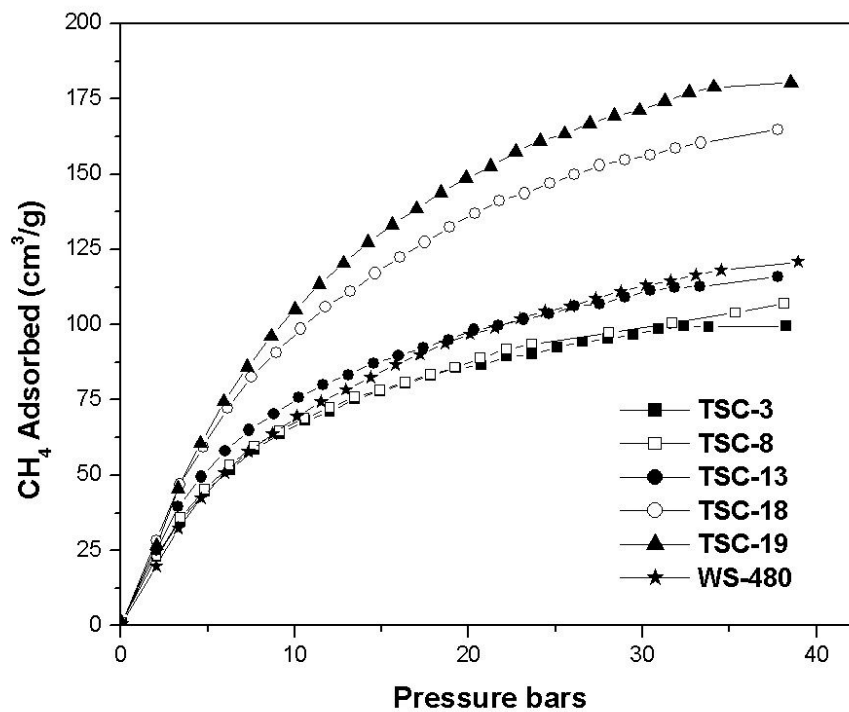


**Fig. 8.** High pressure (up to 35 bars) methane adsorption isotherms at 30°C on TSC samples

**Table 3.** Reported Values of Methane Adsorption Capacity of Activated Carbons Derived from Different Sources

Sr. no	Material	Surface area (m <sup>2</sup> /g)	Methane uptake (mmol g <sup>-1</sup> )	Reference
1	Carbon molecular sieve	1098	4.98	Liu et al. 2006.
2	Activated carbon (resin)	1874	8.60	Sun et al. 2009.
3	Activated carbon fiber (resin)	800	4.92	Sun et al. 2009.
4	Granular Activated Carbon (H <sub>3</sub> PO <sub>4</sub> Activation) Coconut shell	-----	8.43	Prauchner et al. 2008
5	Granular Activated Carbon (ZnCl <sub>2</sub> Activation) Coconut shell	-----	7.54	Prauchner et al. 2008
6	Activated carbon from anthracite	>2500	12-14	Lozano-Castello et al. 2002

## CONCLUSIONS

1. Activated carbon prepared from tamarind seeds (TSC), an agricultural byproduct and waste, showed better methane adsorption capacity as compared to that of commercial activated carbon WS-480. Thus, it could be recommended for methane storage in India in place of commercial activated carbon.
2. For obtaining a methane adsorption capacity of about 32 cm<sup>3</sup>/g, the chemical activation of tamarind seeds with T-char to KOH ratio 1: 4, activation temperature 600-700 °C and 60 minutes activation time is required.
3. It was observed that the textural properties such as surface area and micropore volume mainly govern the methane adsorption capacity.
4. Tamarind seeds are an alternate biomass/agro-byproduct and waste that has potential to be used for the production of activated carbon.
5. Results of high pressure adsorption measurement showed a methane adsorption capacity of 180 cm<sup>3</sup>/g at 35 bars.

## ACKNOWLEDGEMENTS

The authors are grateful to Bharat Petroleum Corporation Limited, CRDC, Noida, for their financial support through IISc, Bangalore, India. The authors are thankful to Analytical Science Division of CSMCRI, Bhavnagar, is for their help in instrumental characterization.

**REFERENCES CITED**

- Alcaniz-Monge, J., De la Casa-Lillo, M. A., Cazorla-Amoros, D., and Linares-Solano, A. (1997). "Methane storage in activated carbon fibers," *Carbon*. 35, 291-297.
- Arami-Niya A., Daud, W. M. A. Wan, and Mjalli, F. S. (2010). "Production of palm shell -based activated carbon with more homogeneous pore size distribution," *J. Applied Sciences*. 10(24), 3361-3366.
- Aukett, P. N., Quike, N., Riddiford S., and Tennison, S. R. (1992). "Methane adsorption on microporous carbons – A comparison of experiment, theory, and simulation," *Carbon* 30, 913-924.
- Balsi, S., Dogu, T., and Yucel, H. (1994). "Characterization of activated carbon produced from almond shell and hazelnut shell," *J. Chemical. Technol. and Biotech.* 60, 419-426.
- Bansal, R. C., Donnet, J. B., and Stoeckeli, F. (1988) *Active Carbon*, New York: Marcel Dekker.
- Boonamnuayvitaya, V., Sae-Ung S., and Tanthapanichakoon, W. (2005). "Preparation of activated carbons from coffee residue for the adsorption of formaldehyde," *Separation Purification Technol.* 42, 159-168.
- Bouchelta, C., Medjram, M. S., Bertrand O., and Bellat, J. P. (2008), "Preparation and characterization of activated carbon from date stones by physical activation with steam," *J. Anal. Applied Pyrolysis* 82, 70-77.
- Byrne, J. F, and Marsh, H. *Porosity in Carbons: Characterization and Application* (Edward Patric, J.W.), Edward Arnold, Auckland, New Zealand; (1995) [Chapter 9].
- Caturla, F., Molina-Sabio, M., and Rodriguez-Reinoso, F. (1991). "Preparation of activated carbon by chemical activation with  $ZnCl_2$ ," *Carbon*. 29, 999-1007.
- Chen, X. S., McEnaney, B., Mays, T. J., Alcaniz-Monge, J., Cazorla-Amoros, D., and Linares-Solano, A. (1997). "Theoretical and experimental studies of methane adsorption on microporous carbons," *Carbon*. 35, 1251-1258.
- Cracknell, R. F., Gordon, P., and Gubbins, K. E. (1993). "Influence of pore geometry on the design of microporous materials for methane storage," *J. Phys. Chem.* 97, 494-499.
- Daud, W. M. A. W., and Ali, W. S. W. (2004). "Comparison on pore development of activated carbon produced from palm shell and coconut shell," *Bioresources Technol.* 93, 63-69.
- Gratuito, M. K. B., Panyathanmaporn, T., Chumnanklang, R. A., Sirinuntawittaya, N., and Dutta, A. (2008). "Production of activated carbon from coconut shell: Optimization using response surface methodology," *Bioresources Technol.* 99, 4887-4895.
- Gergova, K., Petrov, N., and Eser, S. (1994). "Adsorption properties and microstructure of activated carbons produced from agricultural by-products by steam pyrolysis," *Carbon*. 32, 693-703.
- Golovoy, A. (1983). "Proceedings: Compressed Natural Gas," Society of Automotive Engineers: Pittsburgh, PA.
- Demirbas, E., Kobya, M., Senturk, E., and Ozkan, T. (2004). "Adsorption kinetics for the removal of chromium(VI) from aqueous solutions on the activated carbons prepared

- from agricultural wastes,” *Water SA* 30, 533-539.
- Laine, J., and Calafat, A. (1991). “Factors affecting the preparation of activated carbons from coconut shell catalyzed by potassium,” *Carbon*. 29, 949-953.
- Lillian-Gomez, M. J., Garcia-Garcia, A, Salinas-Martinez de Lecea, C., and Linares-Solano, A. (1996). “Activated carbons from Spanish coals. 2. Chemical activation,” *Energy and Fuels*. 10, 1108-1114.
- Lillo-Rodenas, M. A., Lozano-Castello, D., Cazorla-Amoros, D., and Linares-Solano, A. (2001). “Preparation of activated carbons from Spanish anthracite. II. Activation by NaOH,” *Carbon*. 39, 751-759.
- Lozano-Castello, D., Lillo-Rodenas, M. A., Cazorla-Amoros, D., and Linares-Solano, A. (2001). “Preparation of activated carbons from Spanish anthracite. I. Activation by KOH,” *Carbon*. 39, 741-749.
- Lozano-Castello, D., Cazorla-Amoros, D., Linares-Solano, A., and Quin, D. F. (2002). “Influence of pore size distribution on methane storage at relatively low pressure: Preparation of activated carbon with optimum pore size,” *Carbon*, 40, 989-1002.
- Matranga, K. R., Myers, A. L., and Glandt, E. D. (1992). “Storage of natural gas by adsorption on activated carbon,” *Chem. Eng. Sci.* 47, 1569-1579.
- Menon, V. C., and Komarneni, S. (1998). “Porous adsorbents for vehicular natural gas storage: A review,” *J. Porous Mater.* 5, 43-58.
- Moreno-Castilla, C., Carrasco-Marn, F., Lopez-Ramon, M. V., and Alvarez-Merino, M. (2001). “Chemical and physical activation of olive-mill waste to produce activated carbons,” *Carbon*. 39, 1415-1420.
- Nakagawa, Y., Molina-Sabio, and Rodriguez-Reinoso, (2007). “Modification of the porous structure along the preparation of activated carbon monoliths with H<sub>3</sub>PO<sub>4</sub> and ZnCl<sub>2</sub>,” *Microporous Mesoporous Mater.* 103, 29-34.
- Otto, K. (1981). “Adsorption of methane on active carbon and zeolite,” In: *Alternative Energy Sources IV*, Vol. 6, Veziroglu, T. N., Ed.; Ann Arbor Science Publishers, Butterworths: Stoneham, MA, 1982; Vol. 6, pp. 241-260.
- Pandolfo, A. G., Amini-Amoli, M., and Killingley, J. S. (1994). “Activated carbons prepared from shells of different coconut varieties,” *Carbon*. 32, 1015-1019.
- Parkyns, N. D., and Quinn, D. F. (1995). “Natural gas adsorbed on carbon,” In: Patrick J.W., editor, *Porosity in Carbons*, Edward Arnold, 293-325.
- Prauchner, M. J., and Rodriguez-Reinoso, F. (2008). “Preparation of granular activated carbons for adsorption of natural gas,” *Microporous Mesoporous Mater.* 109, 581-584.
- Quinn, D. F., MacDonald, J. A., and Sosin, K. (1994). “Microporous carbons as adsorbents for methane,” *Proceedings of the 207th National Meetings of the American Chemical Society*, San Diego, CA; American Chemical Society: Washington, DC.
- Quinn, D. F., and MacDonald, J. A. (1992). “Natural gas storage,” *Carbon*. 30, 1097-1103.
- Ranjan, D., and Hasan, S. H. (2010). “Rice bran carbon: An alternative to commercial activated carbon for the removal of hexa valent chromium from aqueous solution,” *BioResources* 5(3), 1661-1674.
- Rodriguez-Reinoso, F., and Molina-Sabio, M. (1992). “Activated carbons from

- lignocellulosic materials by chemical and/or physical activation,” *Carbon*. 30, 1111-1118.
- Rouquerol, F., Rouquerol J., and Sing K. (1999). *Adsorption by Powders and Porous Solids: Principles, Methodology and Applications*. Academic Press, London.
- Rubel, A. M., and Stencel, J. M. (2000). “CH<sub>4</sub> storage on compressed carbons,” *Fuel*. 79, 1095-1100.
- Sentorun-Shalaby, C., Ucak-Astarlioglu, M. G., Artok, L., and Sarici C. (2006). “Preparation and characterization of activated carbons by one-step steam pyrolysis/activation from apricot stones,” *Microporous Mesoporous Mater.* 88, 126-134.
- Sing, K. S. W., Everett, D. H., Haul, R. A. W., Mascou, L., Pierotti, R. A., and Rouquerol, J. (1985). “Reporting physisorption data for gas/solid systems with special reference to the determination of surface area and porosity,” *Pure and Applied Chemistry* 57, 603-619.
- Srinivasa Kannan, C., and Abu Bakar, M. Z. (2004). “Production of activated carbon from rubber wood sawdust,” *Biomass and Bioenergy* 27, 89-96.
- Sun, Y., Liu, C., Su, W., Zhou, Y., and Zhou, L. (2009). “Principles of methane adsorption and natural gas storage,” *Adsorption*, 15, 133-137.
- Teng, H. J., and Lin, H. C. (1998). “Activated carbon production from low ash sub-bituminous coal with CO<sub>2</sub> activation,” *American Institute of Chemical Eng.* 44, 1170.
- Teng, H., and Hsu, L. (1999). “High- porosity carbons prepared bituminous coal with potassium hydroxide activation,” *Ind. Eng. Chem. Res.* 38, 2947-2953.
- Vasil’ev, L. L., Kanonchik, L. E., and Mishkinis, D. A. (1999). “Vehicular applications of solid sorbents for natural gas storage,” *J. Eng. Phys. Thermophys.* 72, 884-890.
- Yang, T. and Lua A. C. (2006). “Textural and chemical properties of zinc chloride activated carbons prepared from pistachio-nut shells,” *Mater. Chem. Physics*, 100, 438-444.

Article submitted: August 7, 2010; Peer review completed: September 11, 2010; Revised version received: December 16, 2010; Accepted: December 24, 2010; Published: December 28, 2010.